Supporting Information

Structural Determination of a Filamentous Chaperone to Fabricate Electronically Conductive Metalloprotein Nanowires

Yun X. Chen[1], Nicole L. Ing[2], Fengbin Wang[3], Dawei Xu[4], Nancy B. Sloan[4], Nga T. Lam[1], Daniel L. Winter[1], Edward H. Egelman[3], Allon I. Hochbaum[2,5,6], Douglas S. Clark[4,7], and Dominic J. Glover[1*]

[1]School of Biotechnology and Biomolecular Sciences, University of New South Wales, Sydney, NSW 2052, Australia

[2]Department of Materials Science and Engineering, University of California, Irvine, CA 92697, USA

[3]Department of Biochemistry and Molecular Genetics, University of Virginia, Charlottesville, VA 22908, USA

[4]Department of Chemical and Biomolecular Engineering, University of California, Berkeley, CA 94720, USA

[5]Department of Chemistry, University of California, Irvine, CA 92697, USA

[6]Department of Chemical and Biomolecular Engineering, University of California, Irvine, CA 92697, USA

[7]Molecular Biophysics and Integrated Bioimaging Division, Lawrence Berkeley National Laboratory, 1 Cyclotron Road, Berkeley, CA 94720, USA

Table of Contents

Supporting Figures

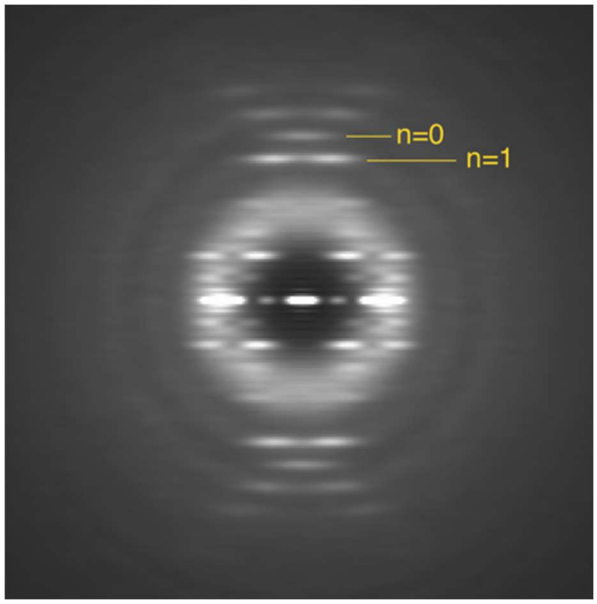

Figure S1. A power spectrum generated from approximately 17,000 overlapping segments of γPFD. The n=0 layer line is at a height of 1/(18 Å).

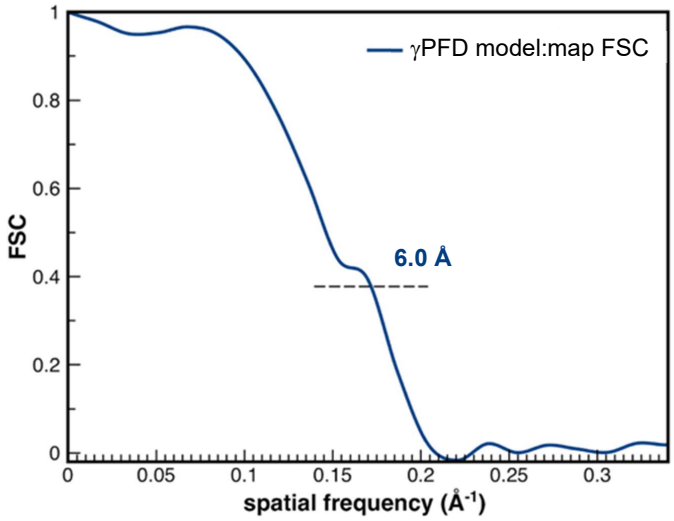

Figure S2. The Fourier shell correlation between the atomic model and the cryo-EM map. The estimated map resolution is 6.0 Å.

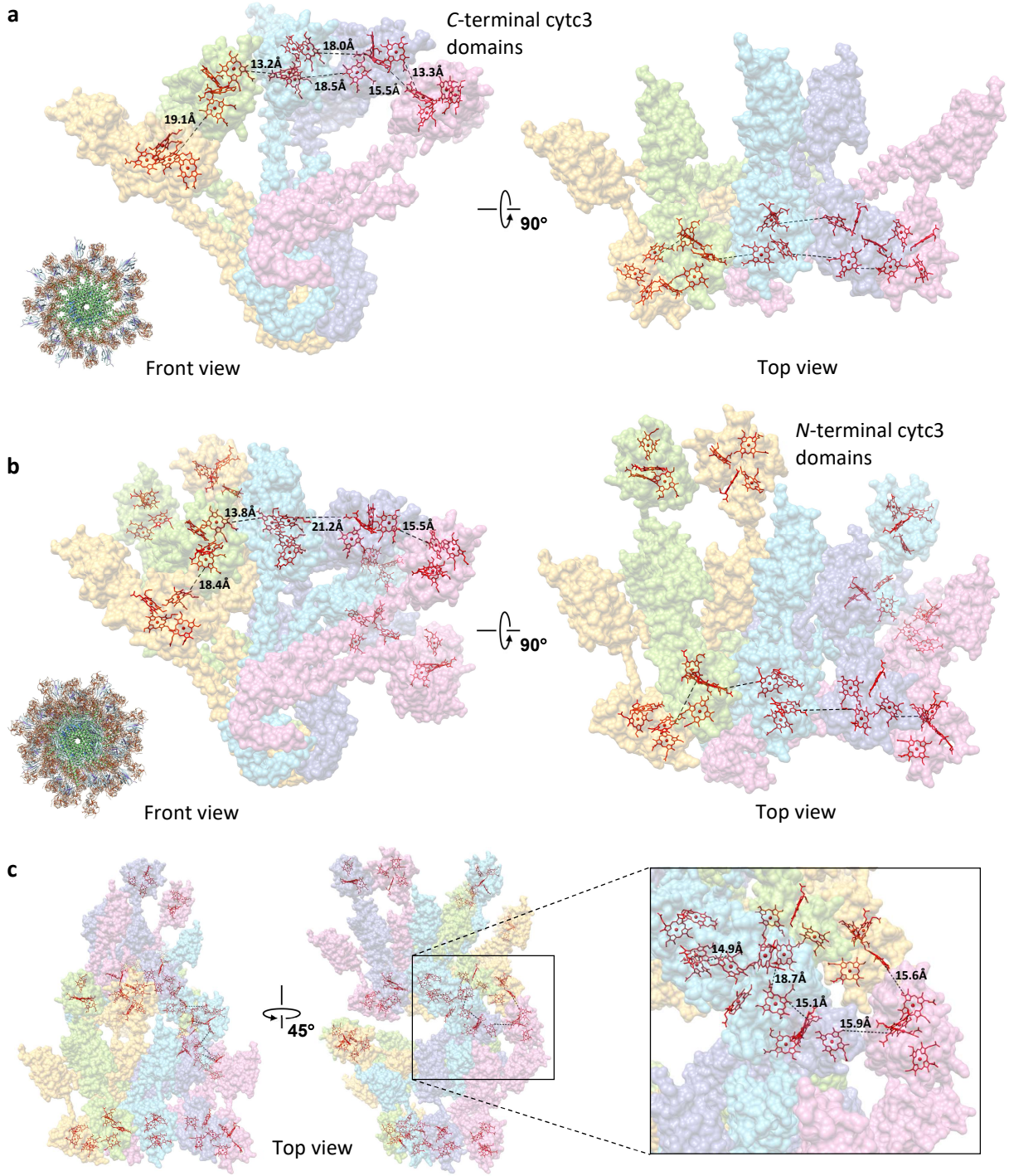

Figure S3. Proposed spatial alignment of hemes in γPFD-metalloprotein nanowires. Minimum observed edge-to-edge distances indicated between the hemes of the *C*-terminal cytochrome c (cytc3) domains of five subunits of the **a**) γPFD-cytc3 and **b**) γPFD-$[cytc3]_2$ nanowires. The helical filament assembly results in a helical alignment of hemes along the length of the nanowire. **c**) The spatial alignment of *N*-terminal and *C*-terminal cytc3 heme domains within the γPFD-$[cytc3]_2$ nanowire. The five γPFD-$[cytc3]_2$ in **b** are shown with five additional subunits that are further along the filament. The minimum observed edge-to-edge distances indicated between hemes of *C*-terminal cytc3 domains and hemes of *N*-terminal cytc3 domains of adjacent subunits. Most of the helical-aligned subunits are hidden for clarity.

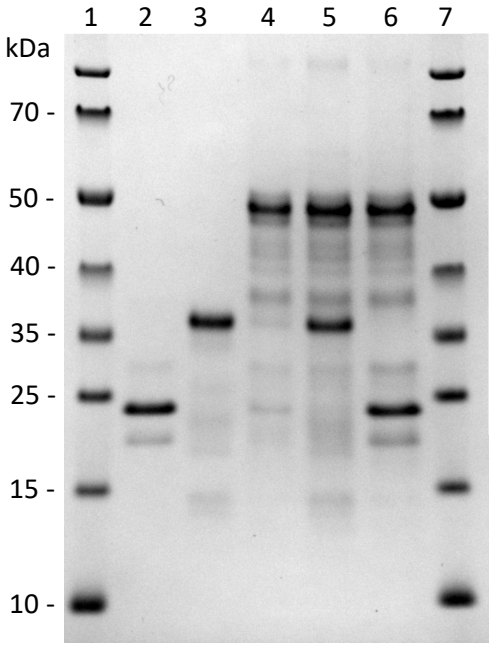

Lane:

1. Spectra multicolor broad range protein ladder
2. γPFD-SpyTag
3. Cytc3-SpyCatcher
4. 1:1 molar ratio of γPFD-SpyTag to cytc3-SpyCatcher
5. 1:2 molar ratio of γPFD-SpyTag to cytc3-SpyCatcher
6. 2:1 molar ratio of γPFD-SpyTag to cytc3-SpyCatcher
7. Spectra multicolor broad range protein ladder

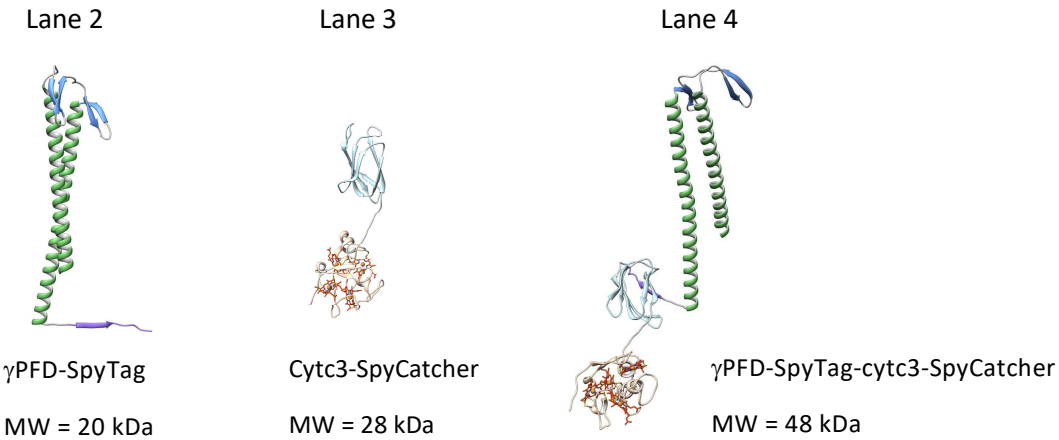

Figure S4. SDS-PAGE gel showing the conjugation of cytc3-SpyCatcher subunits to γPFD-SpyTag at varying molar ratios. At a molar ratio of 1:1 of γPFD-SpyTag to cytc3-SpyCatcher a conjugation product was observed at the expected 48 kDa size. Protein models are included below the gel to represent the expected protein contents in lanes 2-4.

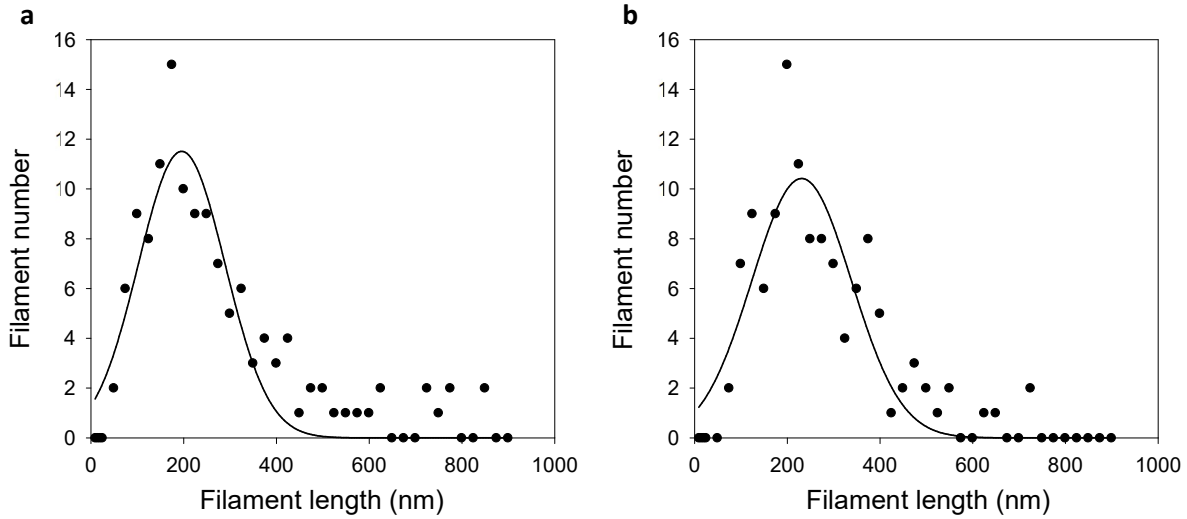

Figure S5. Distribution of γPFD-metalloprotein nanowires lengths. The length of **a**) γPFD-cytc3 and **b**) γPFD-$[cytc3]_2$ nanowires were measured in digitized TEM images and plotted as distribution. (*n* = 130 nanowires).

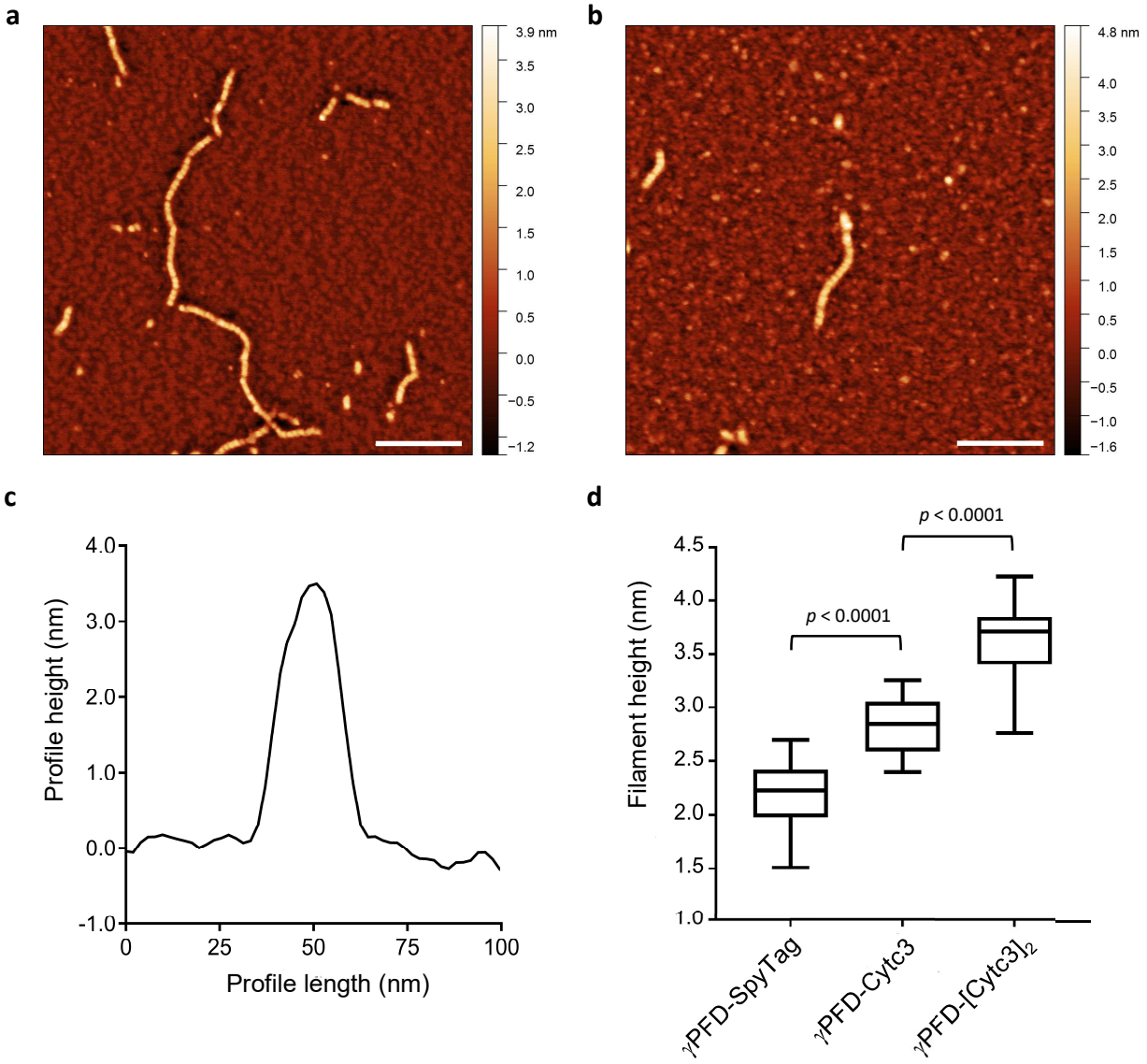

Figure S6. Atomic force microscopy (AFM) imaging of the metalloprotein nanowires. AFM images of **a**) γPFD-cytc3 and **b**) γPFD-$[cytc3]_2$ nanowires. Both scale bars = 200 nm. **c**) Z-height line-scan across the diameter of a γPFD-cytc3nanowire. **d**) Z-height distributions of γPFD-SpyTag filaments, and γPFD-cytc3 and γPFD-$[cytc3]_2$ nanowires. The box-and-whisker plot showing the percentiles and median of filament and nanowire heights (n = 30). The ends of the boxes define the 25th and 75th percentiles, with the line at the median, and error bars defining the 10th and 90th percentiles. Statistical significance of the mean heights was calculated using the unpaired t-test.

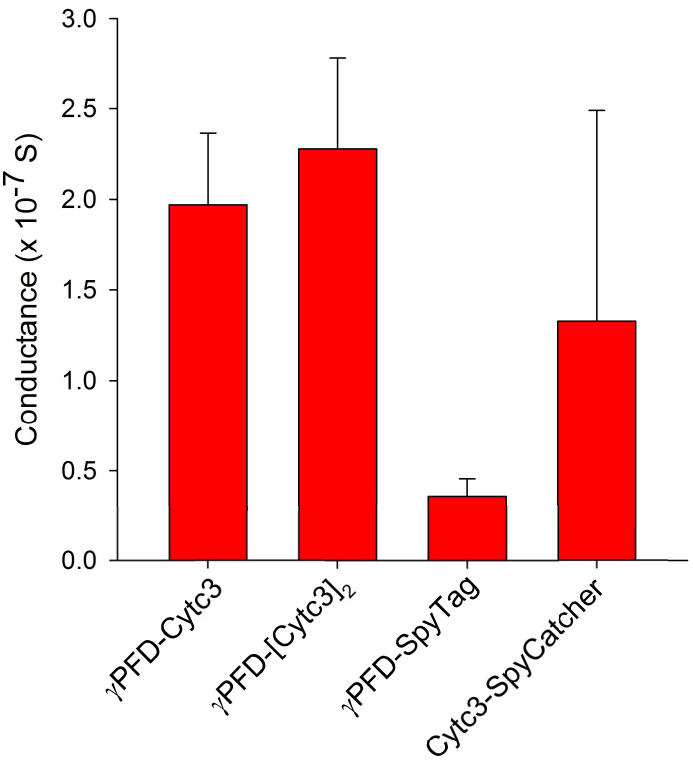

Figure S7. Solid-state conductance measurements of γPFD-cytc3 and γPFD-[cytc3]$_2$ nanowires, and the nanowires individual subunits, γPFD-SpyTag and cytc3-SpyCatcher. Error bars represent standard error of films cast on separate devices (*n* = 3).

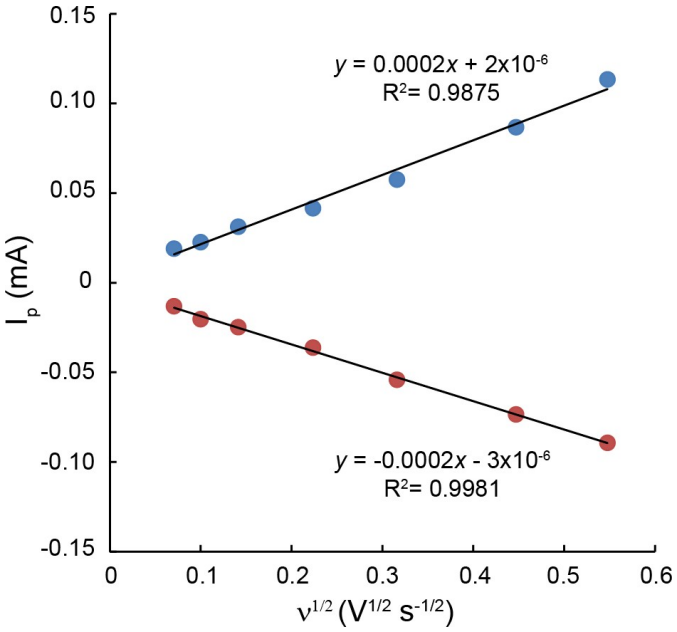

Figure S8. Scan rate analysis of cyclic voltammograms of a representative γPFD-cytc3 film deposited on an IDE device, spanning the source and drain electrodes. Peak current (I_p) values correspond to the peak redox current measured between the source and Pt counter (red) and drain and Pt counter (blue). The potential at the source and drain is swept with respect to an Ag/AgCl reference electrode, with a fixed potential offset V_{DS} maintained between the source and drain working electrodes. The peak current of both electrodes is proportional to the scan rate.

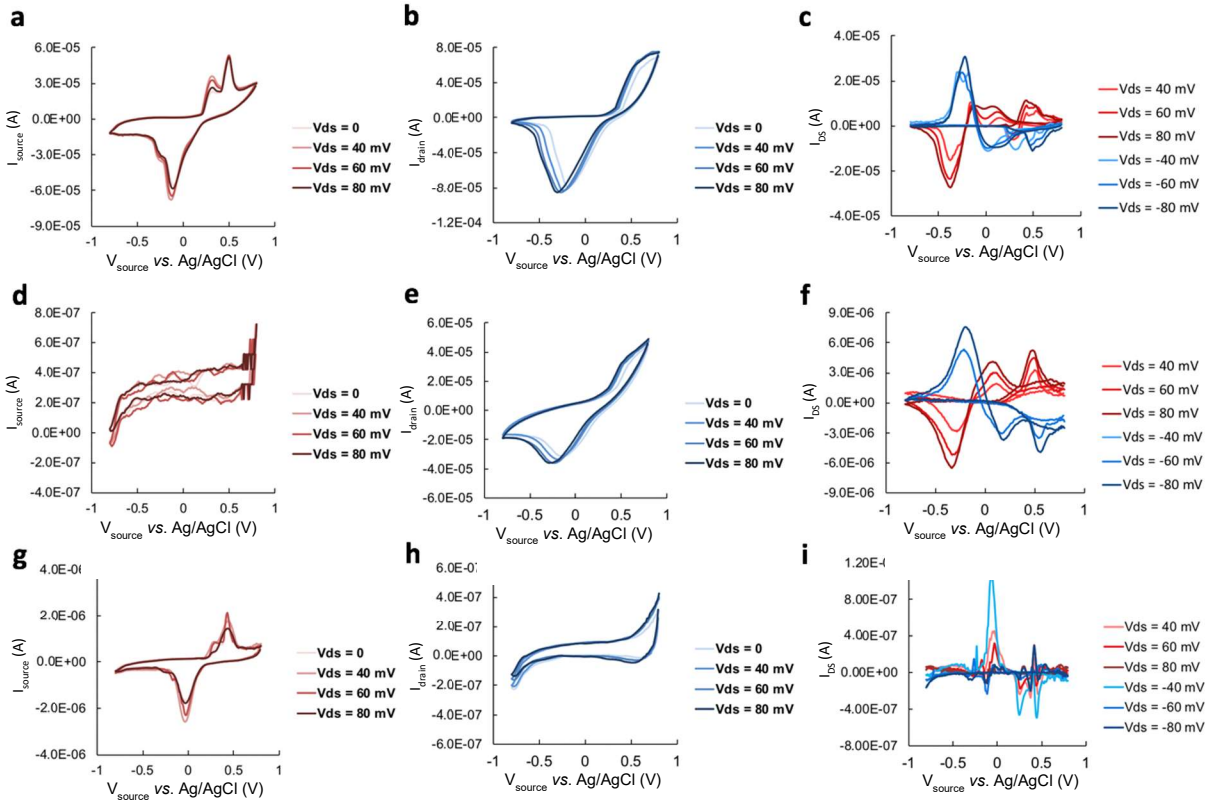

Figure S9. Individual CVs and full (anodic and cathodic) bipotentiostat scans for (**a, b, c**) γPFD-cytc3, (**d, e, f**) cytc3-SpyCatcher, and (**g, h, i**) γPFD-SpyTag films. Raw source (**a, d, g**) and drain (**b, e, h**) CVs at various V_{DS} values reveal distinct redox peaks. Asymmetry in between the source and drain CVs reflects inhomogeneity of film morphology across the device. Since both cytc3 and fibers are short compared to the spacing between electrodes in nature, drying effects may be causing film deposition changes across the deposition spot, affecting percolation network connections. These differences can be normalized by subtracting the values at $V_{DS} = 0$. Subtracting the background-subtracted source and drain currents and halving the difference produces bipotentiostat curves (**c, f, i**).

Supporting Tables

Table S1. Refinement statistics for the γPFD filament model

	γPFD model
Helical symmetry	
Rise (Å)	18.27
Rotation (°)	-48.93
Resolution estimates (Å)	
model:map FSC (0.143/0.38/0.5)	5.3/6.0/6.9
"gold"-standard FSC (0.143)	6.1
d_{99}	6.1
Model *vs*. Data CC	0.88
Clash score, all atoms	6.03
Protein geometry	
Ramachandran favored (%)	91.4
Ramachandran outliers (%)	0
Rotamer outliers (%)	0
Cβ deviations > 0.25 Å	0
RMS deviations	
Bond (Å)	0.004
Angles (°)	0.888
Molprobity score	1.84
PDB ID	6VY1
EMDB ID	EMD-21455

Table S2. Amino acid sequence of γPFD and designed proteins

Protein	**Amino acid sequence**
γPFD	MVNEVIDINEAVRAYIAQIEGLRAEIGRLDATIATLRQSLATLKSLKTLGEGKTVLV PVGSIAQVEMKVEKMDKVVVSVGQNISAELEYEEALKYIEDEIKKLLTFRLVLEQA IAELYAKIEDLIAEAQQTSEEEKAEEEENEEKAE
γPFD-SpyTag	MGHHHHHHENLYFQGGGSMVNEVIDINEAVRAYIAQIEGLRAEIGRLDATIATL RQSLATLKSLKTLGEGKTVLVPVGSIAQVEMKVEKMDKVVVSVGQNISAELEYEE ALKYIEDEIKKLLTFRLVLEQAIAELYAKIEDLIAEAQQTSEEEKAEEEENEEKAEGG GSAHIVMVDAYKPTK
SpyTag-γPFD-SpyTag	MGHHHHHHENLYFQGGGSAHIVMVDAYKPTKGGGSMVNEVIDINEAVRAYIA QIEGLRAEIGRLDATIATLRQSLATLKSLKTLGEGKTVLVPVGSIAQVEMKVEKMD KVVVSVGQNISAELEYEEALKYIEDEIKKLLTFRLVLEQAIAELYAKIEDLIAEAQQT SEEEKAEEEENEEKAEGGGSAHIVMVDAYKPTK
Cytc3-SpyCatcher	MKKTAIAIAVALAGFATVAQAGGGSKKMFLTGVLALAVAIAMPALAAAPKAPA DGLKMDKTKQPVVFNHSTHKAVKCGDCHHPVNGKEDYQKCATAGCHDNMD KKDKSAKGYYHAMHDKGTKFKSCVGCHLETAGADAAKKKELTGCKGSKCHSGG GSVDTLSGLSSEQGQSGDMTIEEDSATHIKFSKRDEDGKELAGATMELRDSSGK TISTWISDGQVKDFYLYPGKYTFVETAAPDGYEVATAITFTVNEQGQVTVNGKA TKGDAHI